

Gravitational arcs as a perturbation of the perfect ring.

C. Alard

Institut d'Astrophysique de Paris, 98bis boulevard Arago, 75014 Paris.

alard@iap.fr

ABSTRACT

The image of a point situated at the center of a circularly symmetric potential is a perfect circle. The perturbative effect of non-symmetrical potential terms is to displace and break the perfect circle. These 2 effects, displacement and breaking are directly related to the Taylor expansion of the perturbation at first order on the circle. The numerical accuracy of this perturbative approach is tested in the case of an elliptical potential with a core radius. The contour of the images and the caustics lines are well re-produced by the perturbative approach. These results suggests that the modeling of arcs, and in particular of tangential arcs may be simplified by using a general perturbative representation on the circle. An interesting feature of the perturbative approach, is that the equation of the caustic line depends only on the values on the circle of the lens displacement field along the θ direction.

Subject headings: gravitational lensing:strong lensing

1. Introduction.

Since the discovery of gravitational arcs in clusters of galaxies by Linds & Petrosian (1986) and subsequently by Soucail *et al.* (1987), the observation and study of arcs has developed considerably, and is now becoming an essential tool in astrophysics. Arcs provides a wealth of information about the mass distribution in clusters of galaxies (see for instance: Comerford *et al.* 2006, & Broadhurst *et al.* 2006). However, the mass distribution of the astrophysical lenses is complex and involves a large parameter space which is difficult to explore. Thus, the derivation of a simplified perturbative theory that is able to re-produce the general features of gravitational arcs is an interesting tool to help understanding complex gravitational lenses.

2. Basic ideas

Let's assume that the projected density of the lens ρ_s is circularly symmetric and centered at the origin. Let's also assume that the lens is dense enough to reach critical density at a given radius R_E . Under such hypothesis, the image by the lens of a point source placed at the origin will be a perfect ring. We are now interested in small perturbations of this perfect ring. There are two type of perturbations to the point source perfectly aligned in a circularly symmetric potential: first the source may not be perfectly at the center, and second the potential may not be perfectly circular. Let's be more specific, in polar coordinates, the lens equation writes:

$$\mathbf{r}_S = \left(\mathbf{r} - \frac{\partial \phi}{\partial r} \right) \mathbf{u}_r - \left(\frac{1}{r} \frac{\partial \phi}{\partial \theta} \right) \mathbf{u}_\theta \quad (1)$$

In the unperturbed case, the equation reads:

$$r - \frac{d\phi_0}{dr} = 0 \quad (2)$$

Where ϕ_0 is a function of r only. Let's now perturb this equation by introducing a small displacement of the source from the origin: \mathbf{r}_s , and a non-circular perturbation to the potential, ψ . Note that the perturbation on r_S and the perturbation on ϕ are assumed to be of the same order. The perturbation may be described by the following formula:

$$\begin{cases} \mathbf{r}_S &= \epsilon \mathbf{r}_s \\ \phi &= \phi_0 + \epsilon \psi \end{cases} \quad (3)$$

Here ϵ is a small number: $\epsilon \ll 1$. Given a position (r_s) for the source, the image positions (r, θ), can be obtained by solving equation (1). However solving directly may prove impossible in the general case. It is easier to find a perturbative solution by inserting Eq. (3) in Eq. (1). Assuming that ϵ is small, the perturbation will introduce a deviation from the perfect circle that will be of order ϵ . An interesting feature of the un-perturbed solution is that the image of a single point at the origin is a full circle, which covers all range in θ . Thus whatever the position θ of the perturbed solution, there is always a point at the same θ in the un-perturbed solution. However, the point in the un-perturbed solution will be located at a slightly different radius r . The response to the perturbation on r may be written, $r = R_E + \epsilon dr$. For convenience, it is always possible to re-scale the coordinate system, so that the Einstein radius is exactly equal to unity, in this case, the perturbation on r is:

$$r = 1 + \epsilon dr \quad (4)$$

To summarize, we must solve perturbatively Eq. (1), by expanding around the un-perturbed solution ($1, \theta$) for small values of ϵ . Note that this requires to expand the potential at $r = 1$.

Using Eq. (3), the Taylor expansion of ϕ may be written:

$$\phi = \phi_0 + \epsilon\psi = \sum_{n=0}^{\infty} [C_n + \epsilon f_n(\theta)] (r-1)^n \quad (5)$$

Where we define,

$$C_n = \frac{1}{n!} \left[\frac{d^n \phi_0}{d^n r} \right]_{(r=1)} \quad (6)$$

And:

$$f_n(\theta) = \frac{1}{n!} \left[\frac{\partial^n \psi}{\partial^n r} \right]_{(r=1)} \quad (7)$$

It is now possible to expand each side of Eq. (1) in series of ϵ , in the vicinity of the unperturbed solution. By inserting Eq. (5), and Eq. (4) in Eq. (1), the response dr to the perturbation defined in Eq. (3) can be estimated to the first order in ϵ .

$$\epsilon \mathbf{r}_s = (1 + \epsilon dr - C_1 - \epsilon 2 C_2 dr - \epsilon f_1) \mathbf{u}_r - \epsilon \frac{\partial f_0}{\partial \theta} \mathbf{u}_\theta$$

Note that Eq. (2) implies that $C_1 = 1$, consequently:

$$\mathbf{r}_s = (\kappa dr - f_1) \mathbf{u}_r - \frac{\partial f_0}{\partial \theta} \mathbf{u}_\theta \quad (8)$$

With: $\kappa = 1 - 2 C_2$.

3. Reconstruction of images.

3.1. Circular source contours.

Let's consider a circular contour on a source with center \mathbf{r}_0 radius, R_0 . The equation for this contour is:

$$(\mathbf{r}_s - \mathbf{r}_0)^2 = R_0^2 \quad (9)$$

Note that effect of the translation by the vector $\mathbf{r}_0 = (x_0, y_0)$ can be taken into account by re-defining f_0 , and f_1 in Eq. (12):

$$\begin{cases} \mathbf{r}_s = (\kappa dr - \bar{f}_1) \mathbf{u}_r - \frac{\partial \bar{f}_0}{\partial \theta} \mathbf{u}_\theta \\ \bar{f}_i = f_i + x_0 \cos \theta + y_0 \sin \theta \quad i = 0, 1 \end{cases} \quad (10)$$

The image by the lens of this contour can be obtained using Eq's. (9) and (10):

$$R_0^2 = (\kappa dr - \bar{f}_1)^2 + \left(\frac{\partial \bar{f}_0}{\partial \theta} \right)^2 \quad (11)$$

Solving Eq. (11), the 2 following solutions for dr can be obtained:

$$dr = \frac{1}{\kappa} \left[\bar{f}_1 \pm \sqrt{R_0^2 - \left(\frac{\partial \bar{f}_0}{\partial \theta} \right)^2} \right] \quad (12)$$

In the above equation the condition for image formation is: $\Delta = R_0^2 - \left(\frac{\partial \bar{f}_0}{\partial \theta} \right)^2 > 0$. The mean position of the 2 contour lines is $\frac{\bar{f}_1}{\kappa}$, and the image width along the radial direction is $\frac{2 \Delta}{\kappa}$.

3.2. Elliptical source contours.

Using Eq. (10) the source Cartesian coordinates writes:

$$\begin{cases} x_s = (\kappa dr - \bar{f}_1) \cos \theta + \frac{d\bar{f}_0}{d\theta} \sin \theta \\ y_s = (\kappa dr - \bar{f}_1) \sin \theta - \frac{d\bar{f}_0}{d\theta} \cos \theta \end{cases} \quad (13)$$

The equation for an elliptical contour aligned with its main axis aligned with the coordinate system is:

$$(1 - \eta) x_s^2 + (1 + \eta) y_s^2 = R_0^2 \quad (14)$$

Using Eq.'s (14) and (13) one obtains:

$$\begin{cases} dr = \frac{1}{\kappa} \left[\bar{f}_1 + \frac{\eta \sin 2\theta}{S} \frac{d\bar{f}_0}{d\theta} \pm \frac{\sqrt{R_0^2 S - (1 - \eta^2) \left(\frac{d\bar{f}_0}{d\theta} \right)^2}}{S} \right] \\ S = 1 - \eta \cos 2\theta \end{cases} \quad (15)$$

3.3. Numerical testing

The accuracy of Eq. (12) has been tested for a source with a circular contour by direct comparison with numerical integration of the lens equation using ray-tracing. For this application, the potential proposed by Blandford & Kochanek (1987) (hereafter, BK1987) was chosen. The asymptotic isothermal form of the potential was selected. The potential reads:

$$\phi = s \sqrt{s^2 + 1} \left[\sqrt{1 + \frac{r^2 (1 - \eta \cos 2\theta)}{s^2}} - 1 \right] \quad (16)$$

The ellipticity of the potential is controlled by the parameter η , BK1987 conclude that for physical reasons η must be less than 0.2. The circular, unperturbed potential ϕ_0 corresponds

to $\eta = 0$, in this case, at $r = 1$, $\frac{\partial\phi}{\partial r} = 1$ which implies that $R_E = 1$. According to Eq's. (6) and (7) the parameters of the perturbative expansion are:

$$\begin{cases} \frac{df_0}{d\theta} = \frac{\sqrt{s^2+1} \eta \sin 2\theta}{\sqrt{s^2+1-\eta \cos 2\theta}} \\ f_1 = \frac{\sqrt{s^2+1}(1-\eta \cos 2\theta)}{\sqrt{s^2+1-\eta \cos 2\theta}} - 1 \\ \kappa = \frac{1}{1+s^2} \end{cases} \quad (17)$$

Using equations (12) combined with Eq. (17) it is possible to trace the 2 lines that describe the image contour. The 2 solutions for dr join at the contour edges. The result is visible in Fig. (1). Note that the large tangential arc is well reproduced by the approximation while there is some offset in the position of the inner image. The problem of the inner image can be corrected using an iterative approach: the perturbative method gives a first guess of the image position, at this initial position one may carry a local Taylor expansion of the potential in order to find a better solution, and the procedure may be iterated again.

3.4. Inverse modelling

Given a system of arcs or arclets it is possible to re-construct the perturbation field. Let's define the arc system to reconstruct as a set of contours, with one contour per image. For each contour a radial line of direction θ intersect the contour in 2 points, r_1 and r_2 (provided that θ is in a suitable range). It is simple to relate these 2 functionals to the fields, f_1 and f_0 of the perturbative approach, in the case of a source with circular contour (Eq. (12)):

$$\begin{cases} \bar{f}_1 = \frac{\kappa}{2} (r_1 + r_2) + C \\ \frac{d\bar{f}_0}{d\theta} = \sqrt{R_0^2 - \frac{\kappa^2}{4}(r_2 - r_1)^2} \end{cases} \quad (18)$$

Where C is a constant term. Note that κ is unknown, actually there is a fundamental degeneracy in κ , only f_1/κ , f_0/κ , and R_0/κ may be determined. By using inner of radial image in the iterative approach mentioned in Sec. (3.3), in some case it might be possible to break the degeneracy on κ . It is clear also that instead of circular contours, one could have considered elliptical one, and Eq. (15) may have been used. In such case, it is just a matter of where to put the complexity, either in the source or the lens, and obviously the judging criteria should be that as a whole the complexity is minimal.

4. Caustics in the perturbative approach.

Caustics are singularities, which are defined by the simple property that the determinant of the Jacobian Matrix J is zero on the caustic lines.

$$J = \frac{\partial x_s}{\partial r} \frac{\partial y_s}{\partial \theta} - \frac{\partial x_s}{\partial \theta} \frac{\partial y_s}{\partial r} = 0$$

The calculation of the Jacobian is straightforward from Eq. (13), it follows that:

$$dr = \frac{1}{\kappa} \left[f_1 + \frac{\partial^2 f_0}{\partial^2 \theta} \right] \quad (19)$$

Note that in this case a shift by a vector \mathbf{r}_0 does not have to be introduced thus, $f_0 = \bar{f}_0$, and $f_1 = \bar{f}_1$. Eq. (19) defines the critical lines. The caustics in the source plane can be obtained by inserting Eq. (19) in Eq. (13):

$$\begin{cases} x_s = \frac{d^2 f_0}{d^2 \theta} \cos \theta + \frac{df_0}{d\theta} \sin \theta \\ y_s = \frac{d^2 f_0}{d^2 \theta} \sin \theta - \frac{df_0}{d\theta} \cos \theta \end{cases} \quad (20)$$

Not that Eq. (20) line depends only on f_0 , which is directly related to the multipole expansion of the potential on the circle. The multipole expansion has also the advantage to relate directly f_0 to the density by the means of the coefficients of the multipole expansion at $r = 1$. Turning now to a numerical application, by inserting the expression of f_0 given in Eq. (17) in Eq. (20) a parametric equation of the caustic line is obtained, the result is presented in Fig. (2). The perturbative calculation of the caustic curve is accurate, this suggests that this approximation may be used to derive general results on caustics. A simple result is that:

$$r_s^2 = \left(\frac{df_0}{d\theta} \right)^2 + \frac{d^2 f_0}{d^2 \theta} \quad (21)$$

Eq. (21) may be integrated over θ , the second term $\frac{d^2 f_0}{d^2 \theta}$ due to periodicity, it follows that the typical size of the caustics is directly related to the variance of $\frac{df_0}{d\theta}$. This result demonstrates that the caustics cross-section, are closely related to the deviations of the potential to circular symmetry, which is confirmed by the numerical analysis of Meneghetti *et al.* (2007).

The author would like to thank J.P. Beaulieu and S. Colombi for reading this paper.

REFERENCES

Blandford, R.D., Kochanek, C.S., ApJ, 1987, 312, 658, (BK1987)

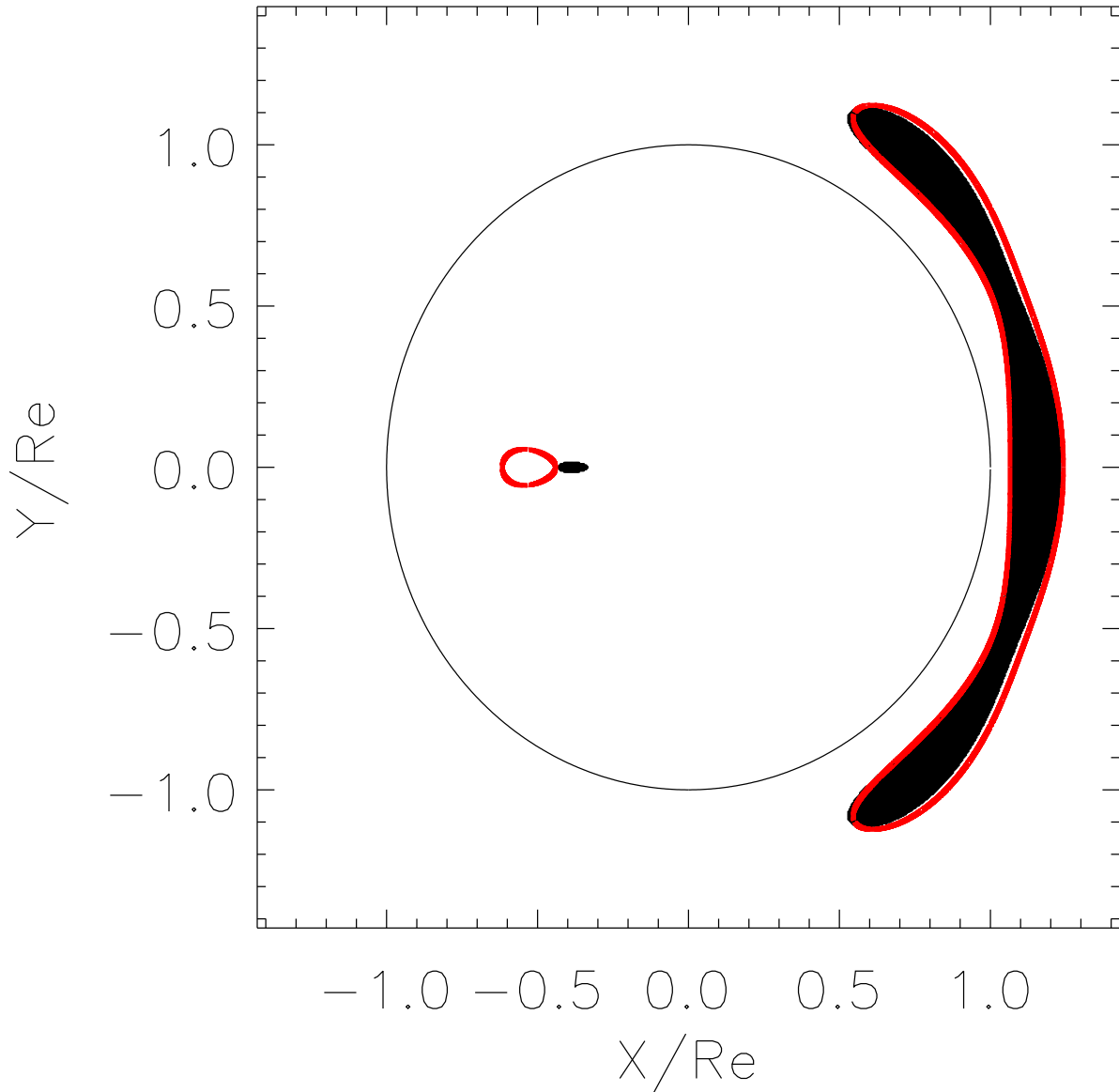


Fig. 1.— A circular source of radius $R_0 = \sqrt{2}/20 R_E$ is placed at $[x_0 = \frac{R_E}{5}, y_0 = 0]$ from the potential center along the X axis. The core radius of the potential is $s = \frac{R_E}{2}$, and the ellipticity is $\eta = \frac{2}{10}$. The dark areas corresponds to the numerical solution obtained by ray tracing. The outer contour of the source is reconstructed using Eq's (12) and (17) and super-imposed (as a red line) on the ray tracing solution. The red contour is close to the outer contour of the ray-tracing solution for the tangential image. Due to the strong non-linearity of the potential near the center, the approximation is not as good for the inner image, although as mentioned in Sec. (3.3) this may be corrected using an iterative approach.

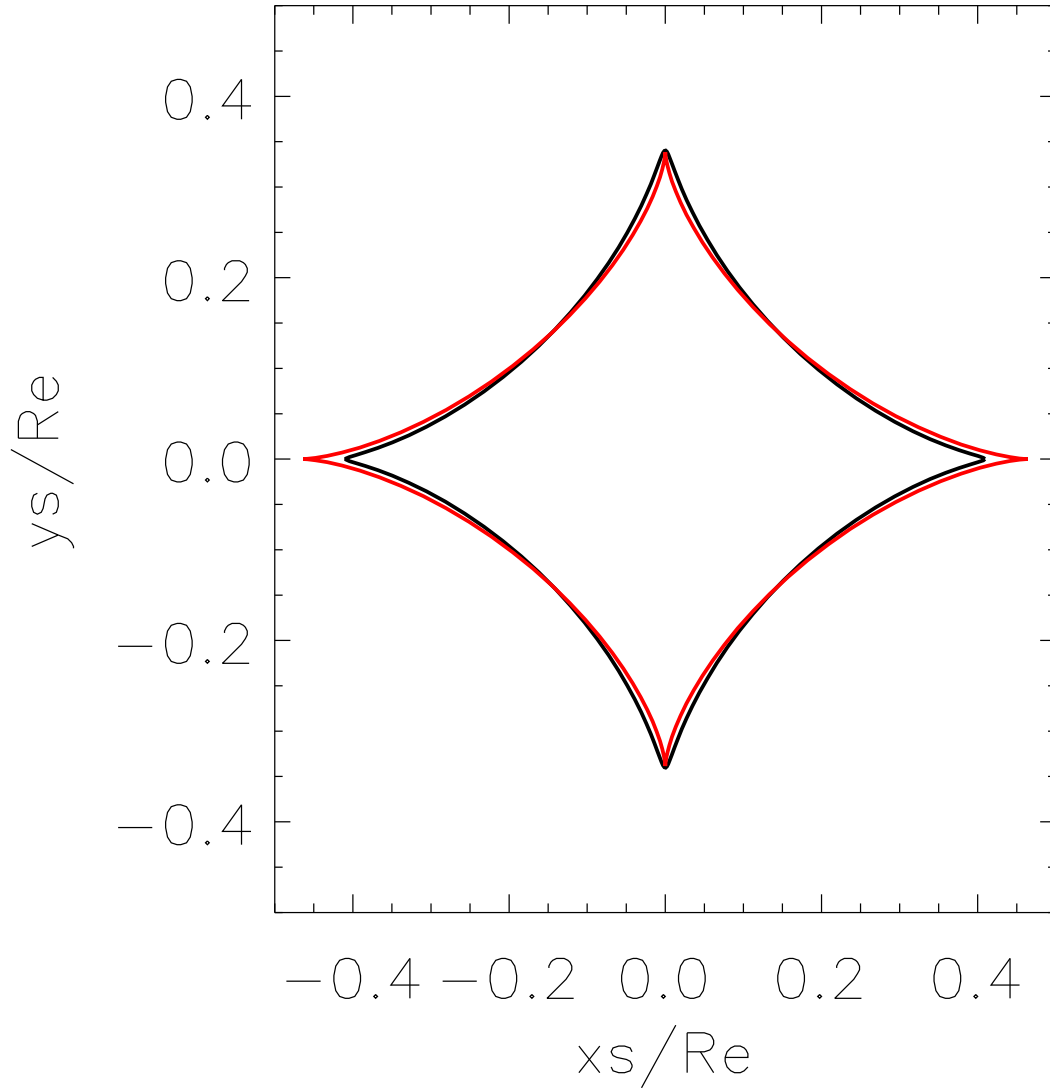


Fig. 2.— Caustics of the BK1987 potential, the perturbative solution is plotted in black next to the numerical solution of the system of equations without approximations. Note the closeness of the 2 solutions.

Broadhurst, T. *et al.*, 2005, *ApJ*, 621, 53

Comerford, J., Meneghetti, M., Bartelmann, M., Schirmer, M., 2006, *ApJ*, 642, 39

Kochanek, C.S., 1991, *ApJ*, 373, 354

Lynds, R., and Petrosian, 1986, *Bull. Am. Astron. Soc.*, 18, 1014

Meneghetti, M., *et al.*, 2007, *A&A*, 461, 25

Soucail, G., Fort, B., Mellier, Y., and Picat, J.P., 1987, *A&A*, 172, L14